

Relational Scene Graphs for Object Grounding of Natural Language Commands

Julia Kuhn, Francesco Verdoja, Tsvetomila Mihaylova, and Ville Kyrki

Abstract—Robots are finding wider adoption in human environments, increasing the need for natural human-robot interaction. However, understanding a natural language command requires the robot to infer the intended task and how to decompose it into executable actions, and to ground those actions in the robot’s knowledge of the environment, including relevant objects, agents, and locations. This challenge can be addressed by combining the capabilities of Large language models (LLMs) to understand natural language with 3D scene graphs (3DSGs) for grounding inferred actions in a semantic representation of the environment. However, many 3DSGs lack explicit spatial relations between objects, even though humans often rely on these relations to describe an environment. This paper investigates whether incorporating open- or closed-vocabulary spatial relations into 3DSGs can improve the ability of LLMs to interpret natural language commands. To address this, we propose an LLM-based pipeline for target object grounding from open vocabulary language commands and a vision language model (VLM)-based pipeline to add open-vocabulary spatial edges to 3DSGs from images captured while mapping. Finally, two LLMs are evaluated in a study assessing their performance on the downstream task of target object grounding. Our study demonstrates that explicit spatial relations improve the ability of LLMs to ground objects. Moreover, open-vocabulary relation generation with VLMs proves feasible from robot-captured images, but their advantage over closed-vocabulary relations is found to be limited.

I. INTRODUCTION

The inherent versatility of human language presents many challenges for robots to comprehend and execute natural language commands. For example, a command such as “bring me the small plate from the table” requires considerable contextual knowledge. To interpret this command correctly, it is necessary to determine which plate and which table the user is referring to. This challenge of linking language commands to the physical world is known as *grounding*, and while seemingly straightforward, it poses a significant challenge for robots.

To improve the abilities for command interpretation of robots, natural language processing (NLP) has gained considerable interest in robotics for several decades. Traditionally, robot commands have been restricted to a closed vocabulary, which relies on a fixed set of predefined terms. Free-form natural language commands are instead open-vocabulary. Large language models (LLMs) are well-suited for understanding open-vocabulary inputs, because they are trained on

This work was supported by the Research Council of Finland (decision 354909). The authors acknowledge the use of the MIDAS infrastructure of Aalto School of Electrical Engineering. J. Kuhn, F. Verdoja, and V. Kyrki are with the School of Electrical Engineering, Aalto University, Espoo, Finland. T. Mihaylova is with the School of Science, Aalto University, Espoo, Finland. Email: {firstname.lastname}@aalto.fi

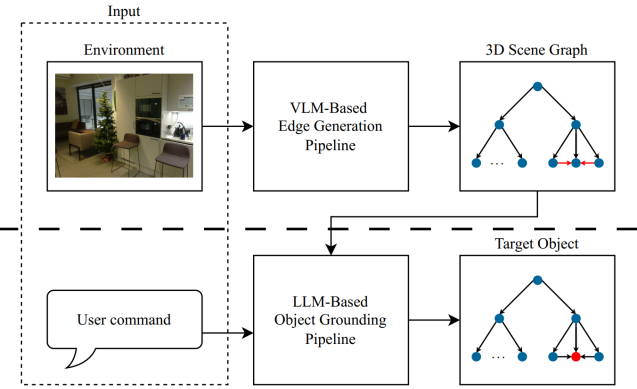


Fig. 1: Based on images captured while mapping, spatial edges are added to a 3D scene graph (3DSG). When a user command is given, the command is grounded through the 3DSG, leveraging the added spatial edges.

vast amounts of human-written text, and their capabilities have steadily increased over the past years. Consequently, their integration into robotics has shown considerable potential [1], [2].

However, grounding language in the environment goes beyond command interpretation and requires perceptual and reasoning capabilities that provide contextual knowledge of the objects and locations referenced in the scene. This knowledge is often recorded in a structured representation, such as a map, tasked to provide both geometric and semantic information. Recently, 3D scene graphs (3DSGs) have been proposed as an effective way to map and subsequently navigate an environment [3], [4]. 3DSGs represent an environment as a graph, with nodes representing entities in the environment (e.g., objects, rooms, and agents), and edges representing the semantic relations between them. While most existing 3DSGs do not record explicit spatial relations between objects (e.g., “the box *under* the bed”), some recent works proposed to encode these spatial relations through edges [5]–[9], given that humans often rely on them to specify objects in an environment. These approaches include both closed-vocabulary edges, some of which are inferred from bounding boxes, and open-vocabulary edges that are inferred from LLMs or vision language models (VLMs). However, it is not known if these edges aid LLMs in parsing 3DSGs to ground objects.

In particular, two questions remain open, which we address in this work:

RQ1 Does incorporating spatial edges improve the ability of

LLMs to ground natural language commands?

RQ2 Considering that these edges are available, which approach to vocabulary yields better performance for the LLMs to ground natural language commands: a closed or open-vocabulary one?

To address the first research question, this paper evaluates the ability of two different LLMs from OpenAI [10], specifically Generative Pre-trained Transformer - 4 omni (GPT-4o) and Generative Pre-trained Transformer - 5 (GPT-5), to utilize spatial relations in 3DSGs for understanding natural language commands. To address the second research question, this paper presents an implementation of an open-vocabulary relation generation pipeline for 3DSGs using a VLM to infer spatial relations, enabling comparison with the closed-vocabulary edges produced by [5]. In Figure 1, an overview of the approaches is shown, where the top line represents the VLM-based edge generation and the bottom line the LLM-based target object grounding.

The main contributions of this paper are:

- An LLM-based pipeline to ground target objects in open-vocabulary commands to an environment represented by a 3DSG.
- A method for extracting and labeling relevant images from the robot's mapping data, which are then used to generate positional edges for 3DSGs through a VLM-based pipeline.
- An extensive study of the performance of two different LLMs tasked to ground target objects in open-vocabulary commands to an environment represented by different 3DSG variations.

II. RELATED WORKS

To operate in the real world, robots benefit from structured models of their environment. There are various ways to represent the environment, and although the more traditional metric maps (*e.g.*, occupancy grid maps [11]) and semantic maps [12] are widely adopted, 3DSGs have found increasing adoption in robotics for their ability to efficiently represent both semantics and structure in a single compact abstraction.

3DSGs represent an environment as a graph. Typically, 3DSGs consist of nodes that represent entities, ranging from objects (with their distinct attributes) to rooms or agents. The nodes are connected through edges that represent the semantic relations between them.

One widely used 3DSG implementation is Hydra [3], which enables real-time scene mapping and subsequent robotic navigation. Real-time Efficient Attribute Clustering and Transfer for Updatable 3D Scene Graph (REACT) [4] extends Hydra by enabling autonomous robots to track and update object states over time. While those 3DSGs offer a solid structural representation of an environment, object-object relations are missing, even though humans often describe objects through them.

3DSGs encode semantic relations as edges between entities. These relations could include spatial relations, preposition and comparative adjective relations, as well as human-object interactions [13].

Spatial relations describe the relative position of two or more entities in 3D space, such as *lamp above bed* or *suitcase between chair and bed*. One approach to extracting spatial relations is to analyze the bounding boxes of detected entities to infer geometric relations, as demonstrated in the Vision and Language-guided Action in 3D Scenes (VLA-3D) dataset [5]. That dataset primarily aims to create a large and diverse collection of indoor scenes, focusing on extracting the 3DSG edges.

Some relations cannot be inferred solely from the objects and their positions. To extract relations that require a deeper understanding of interactions, a growing focus has been on visual relationship detection (VRD) as a research area [13].

Relations can be represented using either closed-vocabulary approaches [5], [6] or open-vocabulary approaches [7]–[9] derived from LLMs or VLMs. Closed-vocabulary relies on a fixed set of predefined terms for each relation type, which simplifies their creation through defined rules, *e.g.*, with bounding boxes. Additionally, using closed-vocabulary relations simplifies the interpretation of the relations. In contrast, open-vocabulary relations instead adhere to natural language by not restricting the choice of words, intuitively enabling more precise and flexible descriptions of the relations between entities. However, it remains an open question whether using open-vocabulary edges helps LLMs on downstream tasks, a topic that this paper aims to investigate. Therefore, this paper presents a study examining whether integrating these spatial relations into REACT 3DSGs benefits LLMs for scene understanding, specifically in the downstream task of target object grounding.

III. PROBLEM FORMULATION

The central problem addressed in this paper is how to enable a robot to accurately identify objects in its environment from natural language referential statements.

In this paper, following the definition in [5], we assume the environment to be represented as a 3DSG, *i.e.*, a graph with nodes that represent objects, including their names and IDs, as well as attributes such as colors and spatial positions in the form of bounding boxes. The relations between the objects are represented through the edges of the graph, containing only spatial edges. These edges are expressed either in closed-vocabulary, *e.g.*, *on*, or in open-vocabulary, *i.e.*, natural language. Both are treated as alternative representations of the same underlying spatial relation. The closed-vocabulary edges are defined unidirectionally from one object to another. An exception to this is the edge *between*, which involves an object positioned in the middle, with the edges pointing unidirectionally to the two associated objects.

A referential statement is a textual description that refers unambiguously to an object in a scene, *e.g.*, “the cabinet that is over the small night stand” is referencing one specific cabinet. Given a referential statement, the task is to identify, within a given 3DSG, the referenced object correctly in terms of its ID.

IV. GROUNDING NATURAL LANGUAGE COMMANDS WITH 3DSGs

The following sections present the proposed solution, which is divided into two parts: grounding natural language commands with the structured 3DSG and enhancing the 3DSG’s expressiveness by refining relations between objects to capture spatial descriptions commonly used in natural language.

A. Enabling LLMs to Reason over 3DSGs

1) *Serializing 3DSGs for LLMs*: A raw 3DSG cannot be interpreted by an LLM and must be converted into a textual representation that includes only the necessary information to interpret the scene. To facilitate the LLM’s processing of the information, both nodes and edges need to be serialized into text.

First, for each node, the object’s name, the unique identifier, and its attributes are converted into string format. Explicitly naming the objects can add semantic context to the scene since the LLM may possess knowledge about particular objects or relations between them from its training data. For instance, an LLM understands that a mug is a small object and that the likelihood of the mug being on the table is greater than it being placed on a chair situated next to the table. The unique identifier (ID) is necessary to distinguish between multiple instances of the same object type. Attributes such as color and size can enhance the LLM’s understanding of the scene, allowing for better differentiation between objects of the same class. Additionally, position information contributes to a general comprehension of the scene.

Second, to make the spatial edges understandable for the LLM, the unique identifiers for the objects along with the corresponding relation between them are used. For the edges in this implementation, the object’s name or other attributes are not considered because they are already present in the nodes and do not provide enough valuable information to warrant the extra space.

2) *Object Grounding with LLMs*: Direct interaction between the LLM and the serialized 3DSG is necessary to ground natural language commands to the objects in the environment. To address this, a pipeline was developed that enables the LLM to query the serialized 3DSG directly, facilitating the grounding of objects in the scene based on natural language commands. An overview of the pipeline structure is shown in Figure 2.

The objective of the pipeline is to query for a particular object in a 3DSG based on a natural language referential statement. It takes two inputs: the processed 3DSG and the natural language command. The two inputs are sent via a prompt¹, which comprises two parts: a system message that defines the behavior of the LLM on a higher level and a user message that contains both the serialized 3DSG and the natural language command. The expected LLM output is the

¹All prompts used are available at https://anonymous.4open.science/r/scenegraph_paper_utils-3A35

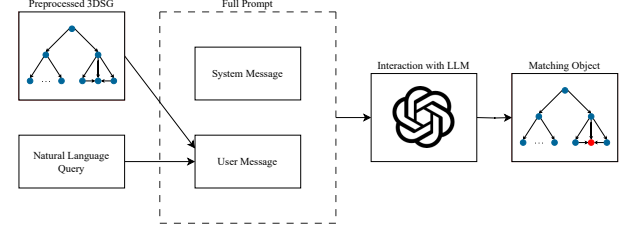


Fig. 2: Overview of the LLM-based pipeline for object grounding in 3DSGs.

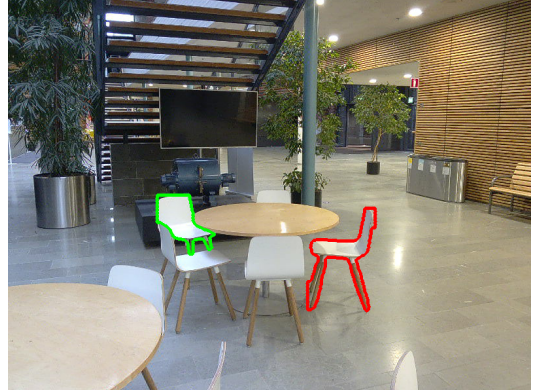


Fig. 3: Example image used for edge generation, where the generated edge is: *both are positioned around the same table, facing each other*

ID of the referenced object that best responds to the query. To avoid biased outputs, prompts are sent without a chat memory. Thus, both the system and the user message are included with every request.

B. Generating Spatial Relations from Visual Data

We implement a VLM-based pipeline to extract relations expressed in natural language between objects from images. We assume that this approach could enhance the 3DSG’s expressiveness by using real-world knowledge of the VLM to integrate richer semantic information into the relations.

1) *Preparing Scene Images for VLM-based pipeline*: To enable the VLM to focus on extracting spatial relations between two objects rather than locating them within the image, a preprocessing step for the images is required. This paper proposes to pre-mark the objects of interest by outlining them in color, ensuring their positions are easily visible to the VLM (e.g., Figure 3). The outlining is done by overlaying segmentation masks over the original image, created by a segmentation model.

Not all 3DSGs contain images of the scenes, which limits this approach to those that do, e.g., REACT [4]. Additionally, it is crucial to identify which exact object is present in each image to generate valid relations.

2) *Inferring Spatial Relations with VLMs*: The pipeline is used to generate spatial relations between objects in the scene by utilizing the preprocessed images. An overview of the pipeline is illustrated in Figure 4.

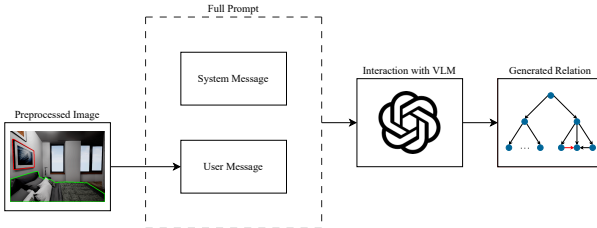


Fig. 4: Overview of the VLM-based pipeline for relation generation.

The system message remains constant for each API request, whereas the user message varies by incorporating an image for the specific relation that should be generated. The output of the VLM consists of the generated relation between the objects in open-vocabulary format. To ensure consistency in format and avoid excessively long edge descriptions, the VLM is instructed to structure and shorten its output. An output example is given in the caption of Figure 3.

V. EXPERIMENTS

The experiments were designed to investigate whether LLMs can leverage spatial edges in 3DSGs. Specifically, Experiment 1 aimed to address RQ1 on the downstream task of target object grounding, while Experiment 2 evaluated whether open-vocabulary edges generated from images impact object grounding performance differently from closed-vocabulary ones (RQ2). We conducted our experiments across two datasets: the VLA-3D dataset [5] and the REACT dataset [4].

A. Evaluation Procedure

Given a 3DSG and a natural language command, the goal was to correctly identify the referenced object in the referential statement. The LLM had to return the ID of the object referenced in the referential statement. To evaluate the LLM performance on this task, the accuracy was calculated by dividing the number of correct predictions by the total number of predictions. A prediction was considered correct when the output ID matched the ground truth ID. Predictions where the LLM output was in an invalid format were counted as incorrect.

To determine whether performance differences between two methods were statistically significant, McNemar's test [14] was employed. This test is well-suited for analyzing paired and binary data.

B. Experimental Setup

1) *Description of VLA-3D Dataset:* The VLA-3D dataset [5] contains 7635 indoor scenes obtained from real-world environments [15]–[19] and scenes synthetically generated with Unity [20]. Each scene contains between 4 and 2264 objects and can be composed of multiple rooms. For each scene, 3D point clouds and object metadata, including bounding boxes, positions, and colors are provided, together

TABLE I: Overview from the used subset of the VLA-3D dataset.

Dataset	Scene Name	Statements
3RScan	0a4b8ef6-a83a-21f2-8672-dce34dd0d7ca	25
	0ad2d3a1-79e2-2212-9b99-a96495d9f7fe	9
	0ad2d3a3-79e2-2212-9a51-9094be707ec2	12
	0ad2d38f-79e2-2212-98d2-9b5060e5e9b5	11
	0ad2d39b-79e2-2212-99ae-830c292cd079	30
	0ad2d39d-79e2-2212-99aa-1e95c5b94289	23
Scannet	scene0000_00	163
	scene0000_01	231
Unity	studio	208
Total		712

with a semantic 3DSGs generated using the procedure described in the VLA-3D paper [21]. These 3DSGs include objects as nodes and their spatial relations as labeled edges. The relation types fall into three categories: binary (*e.g.*, *above*), ordered (*e.g.*, *closest*), and ternary (*e.g.*, *between*). The bounding box information serves as the basis for deriving the relation between the objects. Moreover, for each scene, a list of textual descriptions is provided. Each of these descriptions references a target object and describes it in terms of a specific spatial edge in the scene's 3DSG connecting it to another object. To prevent ambiguous referential statements, the generator appends color or size information when necessary. Although the generated referential statements are semantically rich, the reliance on sentence templates and the use of synonyms limits the linguistic variety.

2) *Preprocessing of VLA-3D Dataset:* The dataset was preprocessed to provide the relevant information in a compact format for the LLM input. From the 3DSGs, we extracted the following attributes for each object: `object_id`, `nyu_label`, `color_labels`, `center`, and `size`. The extracted data allowed the processing of each 3DSG into a compact format suitable for the model, as described in Section IV-A.1. This resulted in an edge format of `obj1_id|relation|obj2_id` for binary and ordered relation types, where `obj1_id` represents the ID of the target object and `obj2_id` represents the ID of the anchor. For the ternary relation type *between*, the target object is between two anchor objects with the ids `obj2_id` and `obj3_id`, which resulted in the edge format `obj1_id|relation|obj2_id and obj3_id`.

A subset of the VLA-3D dataset listed in Table I was used in the evaluation. It comprised nine scenes from three different sources [18]–[20], chosen randomly among real-world and synthetic scenes consisting of a single room. The relations *closest* and *farthest* were excluded from the edges and the referential statements. These relations were defined for every possible pair of objects, creating excessive and often irrelevant relations. To test for a more generalized understanding, we sampled the available referential statements. When multiple synonymous referential statements were available for a single underlying relation, *e.g.*, *below* has synonyms *under* and *beneath*, only one of these

statements was randomly selected. This processing pipeline ensured that only non-redundant and varied referential statements are retained.

3) *Description of REACT Dataset*: The dataset comprises three different real-world indoor scenes captured with Hello Robot Stretch 2 [22]. These scenes are annotated according to the COCO [23] label space, but only for the three most prominent object categories of the scene: chair, couch, and dining table. Furthermore, it contains two synthetically made indoor scenes obtained from the FLAT dataset [24]. In contrast, these scenes had their own label space, with the following object categories: bed, chair, coffee table, floor lamp, journal, picture, sofa, and table.

4) *Preprocessing of REACT*: First, the raw data from the real-world scenes were again processed using the REACT framework to enrich the annotations. The REACT pipeline uses YOLOv11 [25], pre-trained on the COCO dataset, for object detection and instance segmentation. By using the whole COCO label space instead of the three former categories, the number of categories increased to ten. This increased the number and diversity of the relations between the objects.

The 3DSGs produced by the REACT pipeline over the dataset were converted into the VLA-3D format and then passed through the same preprocessing described in Section IV-A.1 to convert the 3DSGs into a format usable by the LLM. Moreover, relational edges and the corresponding referential statements were created for this dataset using the VLA-3D codebase, resulting in 74 referential statements over the five scenes of the dataset.

To generate edges between objects from visual data, images with corresponding highlighted objects were needed, as described in Section IV-B.1. For each detected object, the REACT framework saved the set of images in which the object appeared, along with its corresponding segmentation masks. To find the image in which the two given objects are most visible, all pictures containing both objects were examined. The pixel count for their corresponding segmentation masks was computed, selecting the picture with the highest combined pixel count. Although this approach could fail when object sizes differ greatly, it worked reliably for this dataset.

5) *Creation of REACT Dataset with Human Commands*: In order to extend our evaluation beyond the templated referential statements generated following the VLA-3D approach, we collected statements from human annotators.

For every object in the REACT scenes, the image containing the highest number of pixels belonging to that object was selected and outlined in color. This resulted in 104 images with outlined objects, which were split into 10 batches of 10 or 11 images, and each batch was sent to two different annotators. The following instruction was given to the annotators: “Your friend is in the room shown in the photo. Describe the highlighted object so they can recognize or locate it”. For each object, two descriptions were obtained, resulting in a total of 208 referential statements. The descriptions were then evaluated by the authors for ambiguity. All ambiguous

descriptions (*i.e.*, more than one object in the image matched the descriptions) were discarded, resulting in a final set of 119 statements. We refer to this final set of statements as the *REACT human command dataset*.

6) *Models and Prompt*: In Experiment 1, the models GPT-4o and GPT-5 from OpenAI [10] were used. The system message included an explanation of the task, input and expected output values, a definition of all spatial edges, and an example. The expected output was the ID of the target object specified in the query, which was incorporated into the user message of the prompt. The serialized 3DSG was inserted in the user message. For the model GPT-5, the system and user messages were combined into a single message, because the model expects only one input.

In Experiment 2, GPT-4o was prompted to generate open-vocabulary spatial edges from images. The system message in the prompt included an explanation of the task and the expected output format. The preprocessed image was inserted into the user message, along with the names and IDs of the two objects whose relation was being examined.

C. Experiment 1: Impact of Spatial Edges on LLM Scene Understanding

Experiment 1 was conducted to analyze the difference in LLM scene understanding between a 3DSG with and without spatial edges. Therefore, it investigated whether LLMs can connect spatial edges with positional information from the objects for improved target object grounding.

1) *Experiment design*: To evaluate the impact of spatial edges, three different variants for input graphs were defined: \mathcal{G} , \mathcal{G}_P , and $\mathcal{G}_{P,E}$. \mathcal{G} served as the baseline; it contained only nodes with the object’s name and ID, and no edges. \mathcal{G}_P added color and a bounding box to each node, and $\mathcal{G}_{P,E}$ added the edges of the 3DSG, which represent the relations between the objects.

Because the baseline graph \mathcal{G} contained only the object names, when an object was referenced by name, there was an equal chance for any of the objects with the same name to be retrieved. Therefore, the baseline graph \mathcal{G} was evaluated with the following calculation: For each object class, a set \mathcal{O}_C was created that contained all objects of that specific class. Since objects of the same class could not be distinguished by name alone, the accuracy of each object was calculated by using the probability of randomly selecting the target object from its set \mathcal{O}_C , *i.e.*, $\frac{1}{|\mathcal{O}_C|}$. For the statistical test, one object was randomly selected from \mathcal{O}_C .

The graphs \mathcal{G}_P and $\mathcal{G}_{P,E}$ were both evaluated separately with the pipeline described in Section IV-A.2.

2) *Results*: In Table II, the accuracy of the target object grounding task is shown. For GPT-4o on the VLA-3D dataset, the accuracy improved by 3.97% from \mathcal{G} to \mathcal{G}_P and by 7.3% from \mathcal{G}_P to $\mathcal{G}_{P,E}$, achieving an accuracy of 84.27%. The accuracy on the REACT dataset with GPT-4o increased from the baseline \mathcal{G} to the input graph \mathcal{G}_P by 8.43%. From \mathcal{G}_P to $\mathcal{G}_{P,E}$, an increase of the accuracy of 9.46% can be seen. For GPT-5 on the VLA-3D dataset, $\mathcal{G}_{P,E}$ outperformed \mathcal{G}_P by 1.41% and \mathcal{G} by 26.58% with a total accuracy of

TABLE II: Total accuracy of the target object grounding task for \mathcal{G} , $\mathcal{G}_{\mathcal{P}}$, and $\mathcal{G}_{\mathcal{P},\mathcal{E}}$ on the VLA-3D and REACT datasets.

	Graph	VLA-3D	REACT
Random	\mathcal{G}	0.7300	0.3617
GPT-4o	$\mathcal{G}_{\mathcal{P}}$	0.7697	0.4459
	$\mathcal{G}_{\mathcal{P},\mathcal{E}}$	0.8427	0.5405
GPT-5	$\mathcal{G}_{\mathcal{P}}$	0.9817	0.7297
	$\mathcal{G}_{\mathcal{P},\mathcal{E}}$	0.9958	0.8514

TABLE III: McNemar’s test results for Experiment 1. The significance level was categorized as follows: * significant ($p < 0.05$), ** highly significant ($p < 0.01$), and *** very highly significant ($p < 0.001$).

	Comparison	VLA-3D	REACT
GPT-4o	\mathcal{G} vs $\mathcal{G}_{\mathcal{P}}$		
	\mathcal{G} vs $\mathcal{G}_{\mathcal{P},\mathcal{E}}$	***	**
	$\mathcal{G}_{\mathcal{P}}$ vs $\mathcal{G}_{\mathcal{P},\mathcal{E}}$	***	
GPT-5	\mathcal{G} vs $\mathcal{G}_{\mathcal{P}}$	***	***
	\mathcal{G} vs $\mathcal{G}_{\mathcal{P},\mathcal{E}}$	***	***
	$\mathcal{G}_{\mathcal{P}}$ vs $\mathcal{G}_{\mathcal{P},\mathcal{E}}$	**	*

99.58%. On the REACT dataset, the accuracy was more than doubled when comparing the baseline \mathcal{G} to $\mathcal{G}_{\mathcal{P}}$, and 48.97% higher for $\mathcal{G}_{\mathcal{P},\mathcal{E}}$ compared to \mathcal{G} . For both datasets, edges had a considerable effect on the performance of both LLMs, with GPT-5 outperforming GPT-4o in all cases.

Table III presents the results of McNemar’s test for GPT-4o and GPT-5. For GPT-4o, no statistically significant differences were observed when comparing the baseline \mathcal{G} with the graph $\mathcal{G}_{\mathcal{P}}$. When comparing \mathcal{G} with $\mathcal{G}_{\mathcal{P},\mathcal{E}}$ on both datasets, a statistical significance was shown, from $\mathcal{G}_{\mathcal{P}}$ to $\mathcal{G}_{\mathcal{P},\mathcal{E}}$ only on the VLA-3D dataset. For GPT-5, all differences were statistically significant.

D. Experiment 2: Influence of Open-Vocabulary Edges

In this experiment, the question of whether open-vocabulary spatial edges provide benefits for the LLM-based object grounding compared to the closed-vocabulary ones was investigated.

1) *Experiment Design*: For this experiment, the VLM only generated edges that are also present in the graph $\mathcal{G}_{\mathcal{P},\mathcal{E}}$. This enables using the same referential statements for open and closed-vocabulary edges. If an edge was present in the dataset but could not be estimated because there was no fitting image, the original edge was used instead. This resulted in the input graph $\mathcal{G}_{\mathcal{P},\mathcal{E}}$. Only reference statements with associated edges that were newly generated were tested, which resulted in 26 reference statements. Of these, 22 had the edge *near*, and 4 had the edge *on*. Furthermore, the human-generated commands of the REACT dataset were evaluated.

The same setup as in Experiment 1 was then used with $\mathcal{G}_{\mathcal{P},\mathcal{E}}$ and compared against the results with the input graph $\mathcal{G}_{\mathcal{P},\mathcal{E}}$.



Fig. 5: Example image used for edge generation, where the generated edge is: *left side of the table, closer to the camera*

TABLE IV: Total accuracy of the target object grounding task for $\mathcal{G}_{\mathcal{P},\mathcal{E}}$ and $\mathcal{G}_{\mathcal{P},\bar{\mathcal{E}}}$ on the REACT dataset.

	Graph	Generated Commands	Human Commands
GPT-4o	$\mathcal{G}_{\mathcal{P},\mathcal{E}}$	0.7308	0.4202
	$\mathcal{G}_{\mathcal{P},\bar{\mathcal{E}}}$	0.6923	0.3613
GPT-5	$\mathcal{G}_{\mathcal{P},\mathcal{E}}$	0.8077	0.6218
	$\mathcal{G}_{\mathcal{P},\bar{\mathcal{E}}}$	0.8462	0.5882

2) *Results*: For the closed-vocabulary edge *on*, the open-vocabulary version chosen by the VLM was *on top of*. Several different edges were generated instead of the closed-vocabulary relation *near*. For instance, in Figure 3 and Figure 5, a similar setting was depicted, where two chairs were positioned around the same table. The resulting edges are: *both are positioned around the same table, facing each other* and *left side of the table, closer to the camera*. Other examples for the generated edge from the closed-vocabulary relation *near* included *closer to the glass wall and stairs than* and *near center, in front of a long white table, red chair is far to the back right corner*.

The accuracy on the REACT dataset with generated and human-made referential statements of the graph with the closed-vocabulary edges $\mathcal{G}_{\mathcal{P},\mathcal{E}}$ and the generated open-vocabulary edges $\mathcal{G}_{\mathcal{P},\bar{\mathcal{E}}}$ is shown in Table IV.

On the REACT dataset with the generated commands, the accuracy of $\mathcal{G}_{\mathcal{P},\bar{\mathcal{E}}}$ was 3.7% lower compared to $\mathcal{G}_{\mathcal{P},\mathcal{E}}$ for GPT-4o and 3.85% lower for GPT-5. The same trend was evident in the human-generated statements, where GPT-4o yielded an accuracy decrease of 5.89% and GPT-5 resulted in a 3.36% decrease. These differences in accuracy between the closed-vocabulary edges and the generated edges were not statistically significant.

E. Discussion

The results of Experiment 1 revealed how different LLMs handle 3DSGs for target object grounding. GPT-4o and, especially GPT-5 consistently benefited from the inclusion of spatial edges on the VLA-3D dataset.

For GPT-4o and GPT-5 the performance steadily improved from \mathcal{G} to $\mathcal{G}_{\mathcal{P}}$, as well as from $\mathcal{G}_{\mathcal{P}}$ to $\mathcal{G}_{\mathcal{P},\mathcal{E}}$. This suggests

that these models are capable of reasoning with positional inputs and that spatial edges are beneficial for the LLM to understand object relations. Overall, GPT-5 demonstrated the best accuracy in every category, reaching an impressive 99.5% accuracy on VLA-3D and 85% on REACT.

As a note, the model Generative Pre-trained Transformer - 3.5 (GPT-3.5) was also tested on the VLA-3D dataset, but its accuracy declined as more information was given. This implies that the model struggles to reason with additional information and is even hindered by it. This indicates that for older LLMs, it may be beneficial to reduce the additional information to achieve better performance.

The trend in accuracies observed for the evaluation with GPT-4o and GPT-5 on the VLA-3D dataset was also evident for the REACT dataset, which showed a consistent improvement from the baseline \mathcal{G} to $\mathcal{G}_{\mathcal{P}}$, and from $\mathcal{G}_{\mathcal{P}}$ to $\mathcal{G}_{\mathcal{P},\mathcal{E}}$.

Of the two datasets, the REACT dataset proved the most challenging, with a decrease in accuracy of 30.22% for GPT-4o and 14.44% for GPT-5 for $\mathcal{G}_{\mathcal{P},\mathcal{E}}$ when compared to the VLA-3D dataset. This may be attributed to the more challenging environment, where many objects belonged to the same class and often shared similar attributes (see Figure 3 and Figure 5), resulting in ambiguous edges.

The differences in accuracy between the closed-vocabulary edges and the generated edges from Experiment 2 were not statistically significant, indicating that open-vocabulary relations generated from images neither consistently outperform nor significantly underperform closed-vocabulary relations for the object grounding task. Due to the small scale of the REACT dataset, the lack of statistical significance may partly stem from insufficient data rather than an actual absence of performance difference.

There were both successful and unsuccessful examples of the generated edges. A successful example included the edge *both are positioned around the same table, facing each other*, which resulted in a more precise and semantically meaningful relation. In contrast, an unsuccessful example was the edge *left side of the table, closer to the camera*. This edge was misleading, as the VLM attempted to describe the scene related to the camera position at the time of capture. However, the 3DSG contains no information about the camera or its positions while capturing the scene. Additionally, when viewed from the opposite side of the table, the chairs are positioned to the right of the table, and the chair marked in red would be closer to the observer. This failure suggests that the model struggles to generate view-independent edges.

When no straightforward relation existed between the objects, the model encountered difficulties. As was suggested in the prompt, the model can use other objects to describe the relations between items. For instance, it generated the edge *closer to the glass wall and stairs than*, yet these objects are not part of the 3DSG, making it unclear how these edges compare qualitatively to the closed ones. In some cases, the model generated edges that included the outline colors, *e.g.*, *near center, in front of a long white table, red chair is far to the back right corner*. This presents a problem, as the 3DSG does not contain a *red chair*.

Misleading or incorrectly generated edges can create potential issues, and filtering out these edges can be difficult. The absence of a clear performance gap between the two edge representations suggests that the potential benefits of open-vocabulary relations may currently be limited less by their expressiveness and more by the reliability of their generation.

VI. CONCLUSION

In this paper, we investigated how well LLMs can leverage edges describing object relations in 3DSGs to improve grounding of target objects, and whether open- or closed-vocabulary yields superior performance.

We demonstrated that incorporating explicit spatial information, including both positional information and spatial edges, can improve the performance of LLMs in object grounding tasks. Especially more capable models, such as GPT-5, benefit from this to the point of reaching above 99.5% accuracy on some datasets, compared to the baseline accuracy of 73.0%. Furthermore, no statistically significant difference in performance could be found when using open- or closed-vocabulary edges in 3DSGs for object grounding.

Although no statistically significant performance difference was observed, the result does not rule out the usefulness of open-vocabulary edges. Their current effectiveness may be primarily limited by the reliability of automatic relation generation, making robust and consistent edge extraction a key direction for future work. Beyond relation quality, this approach encounters scalability challenges, as larger scenes consist of more objects and edges between them, which may exceed the LLM’s token limit. Further research could address these limitations by improving the handling of 3DSGs, similar to SayPlan [26], by identifying relevant subgraphs, or borrowing ideas from Retrieval Augmented Generation (RAG) [27]. Furthermore, research could explore other prompt formats and prompting techniques, *e.g.*, chain of thought prompting [28].

By demonstrating how LLMs can effectively leverage spatial edges in 3DSGs for reasoning, this work highlights a promising direction for future robotic systems.

VII. ACKNOWLEDGMENTS

The authors would like to acknowledge the use of Grammarly’s generative AI tool [29] and OpenAI’s GPT4o [10] for improving readability across all sections. Additionally, the authors acknowledge the role of OpenAI’s GPT4o in generating documentation and improving code readability in the project’s code base.

REFERENCES

- [1] W. Huang, P. Abbeel, D. Pathak, and I. Mordatch, “Language models as zero-shot planners: Extracting actionable knowledge for embodied agents,” in *Proceedings of the 39th International Conference on Machine Learning*, ser. Proceedings of Machine Learning Research, K. Chaudhuri, S. Jegelka, L. Song, C. Szepesvari, G. Niu, and S. Sabato, Eds., vol. 162. PMLR, Jul. 2022, pp. 9118–9147. [Online]. Available: <https://proceedings.mlr.press/v162/huang22a.html>

[2] B. Ichter *et al.*, “Do as i can, not as i say: Grounding language in robotic affordances,” in *Proceedings of The 6th Conference on Robot Learning*, ser. Proceedings of Machine Learning Research, K. Liu, D. Kulic, and J. Ichniowski, Eds., vol. 205. PMLR, Dec. 2023, pp. 287–318. [Online]. Available: <https://proceedings.mlr.press/v205/ichter23a.html>

[3] N. Hughes, Y. Chang, and L. Carlone, “Hydra: A Real-time Spatial Perception System for 3D Scene Graph Construction and Optimization,” in *Proceedings of Robotics: Science and Systems*, New York City, NY, USA, Jun. 2022.

[4] P. Nguyen, F. Verdoja, and V. Kyrki, “REACT: Real-time Efficient Attribute Clustering and Transfer for Updatable 3D Scene Graph,” in *2025 IEEE/RSJ International Conference on Intelligent Robots and Systems (IROS)*. IEEE, Oct. 2025.

[5] H. Zhang, N. Zantout, P. Kachana, Z. Wu, J. Zhang, and W. Wang, “VLA-3D: A Dataset for 3D Semantic Scene Understanding and Navigation,” in *2024 Robotics Science and Systems conference (RSS)*, Jul. 2024. [Online]. Available: https://semrob.github.io/docs/rss_semrob2024_cr_paper12.pdf

[6] S. Linok *et al.*, “Beyond bare queries: Open-vocabulary object grounding with 3d scene graph,” in *2025 IEEE International Conference on Robotics and Automation (ICRA)*, 2025, pp. 13 582–13 589.

[7] Q. Gu *et al.*, “Conceptgraphs: Open-vocabulary 3d scene graphs for perception and planning,” in *2024 IEEE International Conference on Robotics and Automation (ICRA)*, 2024, pp. 5021–5028.

[8] D. Rotondi, F. Scaparro, H. Blum, and K. O. Arras, “Fungraph: Functionality aware 3d scene graphs for language-prompted scene interaction,” 2025. [Online]. Available: <https://arxiv.org/abs/2503.07909>

[9] X. Wang, D. Yang, Y. Gao, Y. Yue, Y. Yang, and M. Fu, “Gaussiangraph: 3d gaussian-based scene graph generation for open-world scene understanding,” 2025. [Online]. Available: <https://arxiv.org/abs/2503.04034>

[10] OpenAI, “Models,” 2025, accessed: 05-08-2025. [Online]. Available: <https://platform.openai.com/docs/models>

[11] H. Moravec and A. Elfes, “High resolution maps from wide angle sonar,” in *Proceedings. 1985 IEEE International Conference on Robotics and Automation*, vol. 2, 1985, pp. 116–121.

[12] J. Crespo, J. C. Castillo, O. M. Mozos, and R. Barber, “Semantic information for robot navigation: A survey,” *Applied Sciences*, vol. 10, no. 2, 2020. [Online]. Available: <https://www.mdpi.com/2076-3417/10/2/497>

[13] J. Cheng *et al.*, “Visual relationship detection: A survey,” *IEEE Transactions on Cybernetics*, vol. 52, no. 8, pp. 8453–8466, 2022.

[14] Q. McNemar, “Note on the sampling error of the difference between correlated proportions or percentages,” *Psychometrika*, vol. 12, no. 2, pp. 153–157, 1947.

[15] G. Baruch *et al.*, “ARKitscenes: A diverse real-world dataset for 3d indoor scene understanding using mobile RGB-d data,” in *Thirty-fifth Conference on Neural Information Processing Systems Datasets and Benchmarks Track (Round 1)*, 2021. [Online]. Available: <https://openreview.net/forum?id=tjZjv.qh.CE>

[16] S. K. Ramakrishnan *et al.*, “Habitat-matterport 3d dataset (hm3d): 1000 large-scale 3d environments for embodied ai,” in *Proceedings of the Neural Information Processing Systems Track on Datasets and Benchmarks*, J. Vanschoren and S. Yeung, Eds., vol. 1, 2021. [Online]. Available: https://datasets-benchmarks-proceedings.neurips.cc/paper_files/paper/2021/file/34173cb38f07f89ddbebc2ac9128303f-Paper-round2.pdf

[17] A. Chang *et al.*, “Matterport3d: Learning from rgb-d data in indoor environments,” in *2017 International Conference on 3D Vision (3DV)*, 2017, pp. 667–676.

[18] A. Dai, A. X. Chang, M. Savva, M. Halber, T. Funkhouser, and M. Nießner, “Scannet: Richly-annotated 3d reconstructions of indoor scenes,” in *2017 IEEE Conference on Computer Vision and Pattern Recognition (CVPR)*, 2017, pp. 2432–2443.

[19] J. Wald, A. Avetisyan, N. Navab, F. Tombari, and M. Niessner, “Ric: 3d object instance re-localization in changing indoor environments,” in *2019 IEEE/CVF International Conference on Computer Vision (ICCV)*, 2019, pp. 7657–7666.

[20] Unity Technologies, “Unity,” 2025, accessed: 2 June 2025. [Online]. Available: <https://unity.com/>

[21] H. Zhang, N. Zantout, P. Kachana, Z. Wu, J. Zhang, and W. Wang, “VLA-3D Dataset (GitHub Repository),” 2024, accessed: 2 June 2025. [Online]. Available: <https://github.com/HaochenZ11/VLA-3D>

[22] C. C. Kemp, A. Edsinger, H. M. Clever, and B. Matulevich, “The design of stretch: A compact, lightweight mobile manipulator for indoor human environments,” in *2022 International Conference on Robotics and Automation (ICRA)*, 2022, pp. 3150–3157.

[23] T.-Y. Lin *et al.*, “Microsoft coco: Common objects in context,” in *Computer Vision – ECCV 2014*, D. Fleet, T. Pajdla, B. Schiele, and T. Tuytelaars, Eds. Cham: Springer International Publishing, 2014, pp. 740–755.

[24] L. Schmid *et al.*, “Panoptic Multi-TSDFs: a Flexible Representation for Online Multi-resolution Volumetric Mapping and Long-term Dynamic Scene Consistency,” in *2022 International Conference on Robotics and Automation (ICRA)*. IEEE, May 2022, p. 8018–8024. [Online]. Available: <http://dx.doi.org/10.1109/ICRA46639.2022.9811877>

[25] G. Jocher and J. Qiu, “Ultralytics yolo11,” 2024. [Online]. Available: <https://github.com/ultralytics/ultralytics>

[26] K. Rana, J. Haviland, S. Garg, J. Abou-Chakra, I. Reid, and N. Suenderhauf, “Sayplan: Grounding large language models using 3d scene graphs for scalable robot task planning,” in *Proceedings of The 7th Conference on Robot Learning*, ser. Proceedings of Machine Learning Research, J. Tan, M. Toussaint, and K. Darvish, Eds., vol. 229. PMLR, Nov. 2023, pp. 23–72. [Online]. Available: <https://proceedings.mlr.press/v229/rana23a.html>

[27] P. Lewis *et al.*, “Retrieval-augmented generation for knowledge-intensive nlp tasks,” in *Proceedings of the 34th International Conference on Neural Information Processing Systems*, ser. NIPS ’20. Curran Associates Inc., 2020.

[28] J. Wei *et al.*, “Chain-of-thought prompting elicits reasoning in large language models,” in *Proceedings of the 36th International Conference on Neural Information Processing Systems*, ser. NIPS ’22. Curran Associates Inc., 2022.

[29] Grammarly, Inc., “Grammarly,” 2025. [Online]. Available: <https://www.grammarly.com>